BBA Advances 1 (2021) 100021

Contents lists available at ScienceDirect

BBA Advances

journal homepage: www.sciencedirect.com/journal/bba-advances

The degree and position of phosphorylation determine the impact of toxic and trace metals on phosphoinositide containing model membranes

Weiam Daear [#], Robyn Mundle [#], Kevin Sule, Elmar J Prenner [*]

Department of Biological Sciences, University of Calgary, T2N 1N4 Calgary, Alberta, Canada

ARTICLE INFO

Keywords:
Phosphatidylinositol
Lipid-metal interactions
Model membranes
Membrane fluidity
Liposomes
Lipid domains

ABSTRACT

This work assessed effects of metal binding on membrane fluidity, liposome size, and lateral organization in biomimetic membranes composed of 1 mol% of selected phosphorylated phosphoinositides in each system. Representative examples of phosphoinositide phosphate, bisphosphate and triphosphate were investigated. These include phosphatidylinositol-(4,5)-bisphosphate, an important signaling lipid constituting a minor component in plasma membranes whereas phosphatidylinositol-(4,5)-bisphosphate clusters support the propagation of secondary messengers in numerous signaling pathways. The high negative charge of phosphoinositides facilitates electrostatic interactions with metals. Lipids are increasingly identified as toxicological targets for divalent metals, which potentially alter lipid packing and domain formation.

Exposure to heavy metals, such as lead and cadmium or elevated levels of essential metals, like cobalt, nickel, and manganese, implicated with various toxic effects were investigated. Phosphatidylinositol-(4)-phosphate and phosphatidylinositol-(3,4,5)-triphosphate containing membranes are rigidified by lead, cobalt, and manganese whilst cadmium and nickel enhanced fluidity of membranes containing phosphatidylinositol-(4,5)-bisphosphate. Only cobalt induced liposome aggregation. All metals enhanced lipid clustering in phosphatidylinositol-(3,4,5)-triphosphate systems, cobalt in phosphatidylinositol-(4,5)-bisphosphate systems, while all metals showed limited changes in lateral film organization in phosphatidylinositol-(4)-phosphate matrices. These observed changes are relevant from the biophysical perspective as interference with the spatiotemporal formation of intricate domains composed of important signaling lipids may contribute to metal toxicity.

Introduction

Increasing industrialization exposes humans to metals, resulting in negative health effects [1-4]. The present study focuses on heavy metals such as lead (Pb^{2+}) and cadmium (Cd^{2+}), which play no biological role in the human body, yet are harmful even below a concentration of 10 μg/dL [5-7]. These metals cause the production of reactive oxygen species that result in lipid peroxidation and DNA damage [7]. Manganese (Mn^{2+}) and cobalt (Co^{2+}) are trace metals where Co^{2+} is a coordinating metal for vitamin B_{12} [3], and Mn^{2+} is important for cellular growth and development [8]. Nickel (Ni^{2+}) is found below 10 μM in the blood but its function is still under debate [4, 9]. Exposure to these metals at a concentration above 10 μM is known to be carcinogenic and neurotoxic [3, 4, 6, 10, 11]. Moreover, these essential metals cause oxidative stress above physiological concentrations [7, 12, 13].

Previous studies on the toxic effects of these metals have focused on their interactions with proteins and DNA whereas the interactions with the lipids of cell membranes remain poorly understood. Reports on the effects of Pb^{2+}, Cd^{2+}, Co^{2+}, Ni^{2+}, and Mn^{2+} on erythrocyte membranes and model systems have revealed the importance of electrostatic interactions making anionic lipids prime targets [14-22]. While the initial contact site would be the outer leaflet of the plasma membrane, it has been shown that these metals can use transporters to gain access into the cell [23-25]. Thus, lipids on the inner leaflet should not be dismissed as potential targets. In this work, three representative phosphoinositide lipids (PPIs) were selected based on their important role in many cellular processes.

PPIs constitute only a minor component of most plasma membranes, yet they play a significant role in signal transduction and membrane trafficking. PPIs are an important source of secondary messengers such as inositol-1,4,5-triphosphate (IP_3) and diacylglycerol (DAG), which are involved in the regulation of metabolism, cellular growth and cellular

* Corresponding author.
E-mail address: eprenner@ucalgary.ca (E.J. Prenner).
[#] Both authors contributed equally and are listed in alphabetical order

https://doi.org/10.1016/j.bbadva.2021.100021

Available online 3 August 2021

division [26-29]. In addition to signaling, these lipids are key players in anchoring and activating plasma membrane proteins, including ion channels, through either nonspecific electrostatic interactions or specific coordination with the phosphate groups on the PPIs [30-32]. These lipids contain an inositol ring, which can be phosphorylated and dephosphorylated at the 3', 4', and/or 5' positions by protein kinases and phosphatases, respectively [33]. The rich phosphorylation pattern is important for cytosolic protein docking and generation of important signaling molecules [34]. The presence of a small PPI pool is necessary for cell growth, division, organization, and maintenance of normal biological conditions [35-43].

Phosphatidylinositol (PI) and its phosphorylated species - PPIs, may be a source of locally enhanced surface charge density in the membrane [44] as the charge of phosphatidylinositol-4-phosphate (PIP) under physiological conditions ranges between -2.0 and -3.0 [45] while phosphatidylinositol-4,5-bisphosphate (PIP_2) and phosphatidylinositol-3,4,5-triphosphate (PIP_3) are found at -4.0 and -5.0, respectively [46]. PIP_2 in DOPC systems at 5 mol% ratio was found to hydrogen bond between the proton at position 3 and the vicinal phosphomonoester groups giving it an overall charge of around -4. Interestingly, for PIP_3, at pH of 7, the phosphate group at position 4 was much lower than the phosphate groups in position 3 and 5. However, it was reported that the phosphate in position 4 can hydrogen bond with both 3 and 5 positions giving PIP_3 an overall charge of -5 [46].

PIP is found in plasma, nuclear and Golgi membranes where it is involved in the formation of secretory vesicles and membrane trafficking emanating from the Golgi network targeted to the plasma membrane [35, 37, 47]. PIP and PIP_2 account for nearly 10% of this signal which correlates to 0.5-1% of total phospholipid [48]. PIP_2 is considered one of the main signaling PI lipids due to its ability to generate signaling molecules IP_3 and DAG from the enzymatic cleavage by phospholipase C. It is mainly localized in the plasma and nuclear membranes where it controls several aspects of membrane protein regulation such as surface receptors for signaling molecules and integral proteins involved in generation of secondary messengers [34]. PIP_3 is even more sparse, estimated at 2-5% of PIP_2 [6, 34]. This corresponds to ~0.02-0.05% of the total lipids [6, 34, 49, 50]. PIP_3 is involved in various cellular functions such as cell survival and proliferation [5, 6, 35-37] and is generally located in the plasma and nuclear membranes [35].

In order to better understand potential preferential interactions between various metals and various PPIs, well-defined model systems were used with a specified concentration of PPIs and metal/lipid ratios. The concentration of metal exposure per lipid *in vivo* can vary as the metals are distributed in the body, complexed during metabolism or eliminated. For example, blood and urine Pb^{2+} levels are regularly used to assess how much Pb^{2+} enters the body throughout all routes of exposure. However, they don't reflect metal levels already taken up by cells, organelles or incorporated into the skeleton.

In this work, the metal effect on model membranes were assessed by measuring changes in membrane fluidity; liposome aggregation in bilayer systems, and lateral film organization in monolayers. The total PI lipid content can be as high as 20 mol% of total cellular lipids and consist of ~80% of phosphoinositides, whereas the phosphorylated PPIs contribute much less. Representative and biologically relevant PPIs carrying one, two, or three phosphate groups [6, 51] were selected for this work. While PIP and PIP_2 comprise 2-5 mol% of PPIs, PIP_3 concentrations are lower at 0.05mol% of the PIs [6, 34].

Moreover, metals effects were studied on model membranes comprised of 99% 1-palmitoyl-2-oleoyl-sn-glycero-3- phosphocholine (POPC) and 1mol% PPIs. The zwitterionic phosphatidylcholines (PC) constitute a major structural components of mammalian membranes [12, 52] and have an overall neutral charge due to charge cancelation from the negative phosphate and the positive choline in the lipid headgroup. All experiments were restricted to 100 mM NaCl at pH 7.4 to avoid unspecific metal binding to buffer components [53].

Metal binding to the liposomes was confirmed by zeta potential measurements. Moreover, metal effects were studied by fluorescence spectroscopy utilizing the amphiphilic membrane probe laurdan which readily incorporates into membranes due to its hydrophobic side chain (Fig. 1). Laurdan reports an average change in fluidity from fluctuations in water content in the membrane interface. This is achieved by calculating the Generalized Polarization (GP) based on the emission spectra in rigid and fluid environments [54]. Liposomes are suitable model membranes exhibiting highly consistent GP values to measure membrane fluidity and phase transitions between gel and liquid-crystalline phases [54]. Indeed, Cd^{2+} induced rigidity has been reported for POPC model systems containing 20% phosphatidylinositol-3-phosphate [18]. Moreover, any metal-induced changes to membrane fluidity can be monitored with high accuracy within ±0.005 standard deviation as shown in supplementary material (Table S1). Concurrently, dynamic light scattering (DLS) was utilized to measure the hydrodynamic radii defining the liposomes size and the size distribution within control and metal exposed liposome populations.

Another relevant aspect was the impact of the metals on lipid packing and the lateral membrane organization. This was investigated by analyzing monolayer isotherms in terms of metal induced area/molecule changes as well as their effect on the compressibility of these films [55-57]. Both parameters area reported as an averaged response of the system whereby the POPC bulk does not interact with the metals. Localized metal induced changes to the lateral organization can be visualized in realtime utilizing Brewster angle microscopy (BAM). While the exact distribution of PI molecules between outer and inner leaflet is not known, monolayers allow for a precise control of the lipid composition [58, 59] and have been previously used to study interactions of ions, drugs, or proteins with lipids [58, 60-62]. Furthermore, monolayer images were taken at surface pressures of around 30mN/m. In this pressure range, monolayer and bilayer pressure have been reported to be equivalent [59, 63-65].

The goal of this study was to quantify metal interactions with important PPIs with varying levels of phosphorylation to gauge potential effects on these lipids that could subsequently impact signaling pathways and proper cellular function. Distinct changes of membrane fluidity and drastic changes in the lateral membrane organization were determined by the degree and the position of phosphorylation and the type of the metal ions tested.

Materials and methods

A key factor to consider for such metal experiments is the charge and speciation of the metals under investigation [21]. According to the Visual Minteq modelling software, VMINTEQ 3.1, the investigated metals speciate mostly into positive ions at the physiological conditions of 100 mM NaCl and pH 7.4 [66] (Table 1). Consequently, interactions with negatively charged lipids such as the PIs must be expected.

Liposome preparation and analysis

Lipids were purchased from Avanti Polar Lipids (USA), whereby phosphoinositides were only offered with identical dioleoyl- (DO) side chains. They were weighed and dissolved in 7:3 (v/v) chloroform: methanol mixtures (Table 2). Laurdan in chloroform added at 1:550 laurdan: lipid molar ratio.

Lipid solutions were then vortexed, sonicated and dried under argon forming films on glass vial walls. For details of the handling of PI lipids see the supplementary information. After a minimum of 4 hours under vacuum employed to evaporate the residual solvent, the lipid films were rehydrated in 100 mM NaCl at pH 7.4. The solution was then freeze/thawed 3 times. The lipid suspension was passed 21 times through a Whatman nucleopore 100 nm polycarbonate filter using a mini extruder (Avanti Polar Lipids, USA) to yield the final suspension of unilamellar liposomes. To account for proper lipid solubility, potential dilution or loss of lipids throughout this process, the lipid concentrations (Table 2)

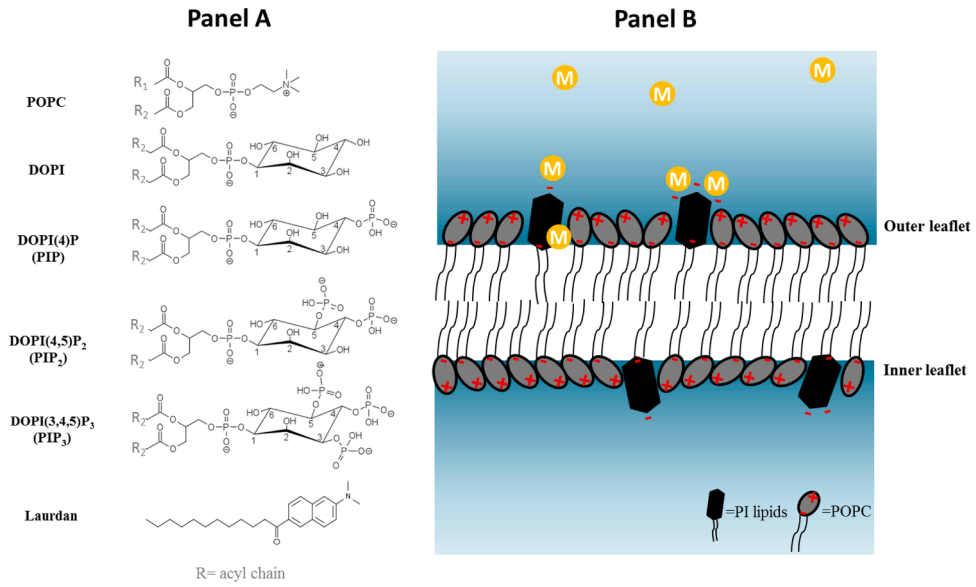

Fig. 1. Schematic illustrations of PI lipids along with potential localization of metal ions in the bulk or bound to the phosphate groups of the PPIs. Panel A) A schematic of the lipid structures used and the fluorescent molecule laurdan. Panel B) Schematic of the proposed metal localization and interaction with PI containing liposomes. R_1 is palmitoyl acyl chain (16:0) and R_2 is oleoyl acyl chain (18:1).

Table 1
The predominant metal species present under physiological conditions of pH 7.4, 100mM NaCl, 37°C as determined by VMINTEQ 3.1 [66].

Metal	% Speciation
Lead	47.4 % $PbCl^+$, 31.9% Pb^{2+}, 13.8% $PbOH^+$, 6.3%$PbCl_2$, 0.5% $PbCl_3^-$
Cadmium	65.2% $CdCl^+$, 18.5% Cd^{2+}, 16.3% $CdCl_2$
Cobalt	98.2% Co^{2+}, 1.6% $CoCl^+$, 0.2% $CoOH^+$
Nickel	98.3% Ni^{2+}, 1.4% $NiCl^+$, 0.3% $NiOH^+$
Manganese	96.1% Mn^{2+}, 3.4% $MnCl^+$, 0.4% $MnCl_2$, 0.1% $MnOH^+$

were determined after extrusion by the Ames assayproviding total phosphate analysis to determine the concentration of inorganic phosphate in solution [67]. To account for pH fluctuations in the unbuffered water used for lipid hydration, the liposome stock solutions were made at higher concentrations (Table 2) and the prepared liposomes were transferred into solutions with proper pH.

Dynamic light scattering (DLS)

The size of liposomes was analyzed by dynamic light scattering technique (DLS) using a Zetasizer Nano ZSP (Malvern Instruments, Worcestershire, UK). The experiments were conducted in triplicates at 25°C. Liposomes at 0.3mM concentration were measured with and without the increasing concentrations of Pb^{2+}, Cd^{2+}, Co^{2+}, Ni^{2+}, and Mn^{2+} to assess any metal induced changes. Furthermore, it was ensured that the size of liposomes was kept at a narrow distribution with a polydispersity index (PDI) of less than 0.10 (< 10%) for each measurement.

Osmolarity of the liposomes was considered and calculated using the osmolarities of the mono- and divalent salts present in the external environment [68]. Briefly, the osmolarity of the mono- and divalent cations were determined based on the number of particles from dissolving the solution in water. The osmolarity of the divalent cation was then divided to the monovalent cation to generate a percentage change in osmolarity.

Liposome size change estimation

Based on an average area/molecule for POPC of around 64.5Å^2 [69, 70], the ratio 51.5% lipids on the outer leaflet [71] and the average diameter of control liposome of 100 nm, it is possible to estimate the average number of lipids in the outer layer as shown on the supplementary material section. Assuming fusion of two vesicles resulting in a larger liposome and consequently a ratio of 51.5% of lipids in the outer layer [71], the radius of the fused liposome would be 708Å, approximately 142 nm in diameter (see Supplementary Material and Fig. S1).

The metal induced changes in molecular area or curvature will affect the size, but the estimate allows to differentiate between liposome swelling (between 100-120 nm), potential fusion (130-150 nm) and aggregation (>140 nm) (Fig. S1).

Laurdan Generalized Polarization (GP)

The emission of the amphipathic probe 6-dodecanoyl-2-dimethylaminonaphthalene (laurdan) is sensitive to the polarity and physical state of the membrane and has been used to monitor membrane fluidity and lipid phase transitions [54]. Fluorescence measurements were performed on a Cary Eclipse spectrofluorometer (Agilent Technologies, USA) by excitation at 340 nm and dual emission readings at 440 nm and 490 nm with 5 nm bandpass each for an average of 4 measurements. GP measurements were conducted at 35°C ±0.1°C using a circulating water bath controller. GP was calculated according to the following equation [54]:

$$GP = \frac{I_{440} - I_{490}}{I_{440} + I_{490}} \quad (1)$$

Table 2
The results of Ames phosphate determination assay for the concentration of lipids post-extrusion [67].

Lipid	Mass (mg)	Lipid	Mass (mg)	Mol % PI	Vol (mL) 7:3 (v/v) $CHCl_3$: MeOH	Conc. Pre-Extrusion (mM)	Conc. Post – Extrusion (mM)
PIP	0.1	POPC	7.74	1.00%	2	5.146	4.49
PIP_2	0.1	POPC	7.15	0.99%	2	4.750	3.51
PIP_3	0.1	POPC	5.36	1.20%	2	3.567	3.40

GP values range between +0.6 to -0.4 depending on a lipid phase state. Under equivalent experimental procedure any changes in laurdan GP upon the addition of metals will correspond to a change in membrane polarity, water accessibility and lipid packing. The change in GP (ΔGP) is calculated as the difference between metal-free controls and fluidity changes in samples containing metals. A decrease (negative values) in ΔGP is an indication of a fluidization effect while an increase (positive values) is an indication of a rigidification effect. The laurdan measurements are highly reproducible within ±0.005, well below the GP increases reported in this manuscript (Table S1).

Control experiments with the water soluble analogue Prodan or Laurdan were performed to exclude spectral changes (such as quenching) upon metal addition and no interferences were observed.

Monolayer studies

PI lipids were dissolved in 7:3 (v/v) chloroform : methanol and mixed with POPC lipids dissolved into 6:4 (v/v) chloroform : methanol to form a 1 mM stock concentration. A Langmuir trough instrument with an area of 200 cm^2 (Biolin, Stockport, UK) was filled with 125 mL of an aqueous subphase (100 mM NaCl, pH 7.4) containing 86.2 μM metals to reach the final 500:1 metal : lipid mol ratio. The films were formed by depositing 21.5μL of 1 mM lipid stock solution onto the air-subphase interface. After a period of 10 minutes, the monolayer was compressed until a surface pressure of 30 mN/m was reached. The images were collected using a Brewster angle microscope (BAM) (Accurion, Germany) and processed by EP3 software (Accurion, Germany). All experiments were conducted at room temperature. The pH stability of the subphase against CO_2 uptake from the air was checked and a decrease in pH values was observed from 7.4 to 7.33 over a period of 60 minutes. This timeline was considerably longer compared to the BAM experiments that never exceeded 30 minutes.

Statistical analysis

Statistical tests were conducted with the 3 replicates for each system using a 2 tailed unpaired T-test in Microsoft Excel. The significance was evaluated at a 95% confidence interval, deemed statistically significant for $p<0.05$.

Results

The initial analysis focused on the impact of the metal ions on membrane fluidity in biomimetic mammalian model membranes composed of POPC and 1 mol% phosphoinositides.

The parent compound, unphosphorylated PI (DOPI) (Fig. 1) carries a single phosphate group that links the inositol ring to the glycerol backbone. Therefore, the negative charge on the phosphate linker of DOPI is less accessible to metals in contrast to the phosphorylated PIs carrying additional phosphate groups. This control was important to ensure that any observed effects are indeed due to presence of extra phosphate groups at the 3', 4', and/or 5' positions, and not due to the bulky nature of the DOPI head group that may affect lipid packing in the binary mixture. The solvent sensitive fluorophore laurdan (Fig. 1) readily inserts into membranes due to its hydrophobic side chain and may be used to detect any changes in polarity at the membrane interface. These changes are often correlated to membrane fluidity [54]. In this work, only minor changes of fluidity were observed for 1 mol% DOPI in POPC upon addition of metals making this lipid system and lipid ratio a suitable platform for further experiments (Fig. S2). All changes were statistically relevant with 95% confidence interval.

Another factor of interest was metal induced liposome aggregation measured by DLS. POPC liposomes served as control membranes and were exposed to the metals resulting in insignificant size changes induced by Pb^{2+} (7.0±0.5 nm) and Mn^{2+} (3 nm) (Fig. 2B). Data for a 1 mol% DOPI system is shown in Fig. S2 with no statistically relevant ΔGP or size changes.

Finally, the lateral monofilm organization in the absence and presence of metals was visualized in real-time by Brewster angle microscopy [62]. The use of monofilms allows a stringent control of the lipid composition and the single layer mimics the outer membrane leaflet interacting with metals in the bulk phase. Fig. S3 shows homogeneous POPC films in the presence of all metals tested. In addition, systems including 1 mol % DOPI also showed very limited domain formation for Cd^{2+} and to an even lesser extent for Ni^{2+} and Mn^{2+}, but no domains for Pb^{2+} or Co^{2+}.

Metal concentrations used were based on values reported in acute exposure studies such as a Danish study finding about 0.3 mM Cd^{2+}, 0.70 mM Co^{2+}, 0.8 mM Pb^{2+}, and 0.4 mM Ni^{2+} in human blood serum [72]. Since the binding affinities of metals are reduced by counter ions, an excess metal/lipid molar ratio of 4:1 was chosen to ensure binding to allow studying the effect of toxicity. In case of Mn^{2+}, 900 μM (or 3:1 metal/lipid) was used because higher stock concentrations would result in precipitation. For monolayer systems, metal concentrations in greater excess of the lipids (500:1 metal: lipid mol ratio) were used to overcome the large subphase volume of 125 mL which can otherwise reduce the interaction of metals with the monolayer.

Each phosphoinositide will be discussed separately to compare the effect of the five metals on the three parameters tested (membrane fluidity, liposome aggregation and domain formation on monolayers).

POPC + 1 mol% PIP (DOPI(4)P)

Statistically significant membrane rigidification based on laurdan measurements was observed upon addition of 1200 μM Pb^{2+} and Co^{2+} with similar ΔGP values of +0.03 ± 0.004 and +0.03 ± 0.004 respectively (Fig. 2A) representing the most pronounced ΔGP changes seen in this work. Cd^{2+}, Ni^{2+}, and Mn^{2+} did not show any statistically significant changes, indicating a weaker effect by these metals. Metal effects on liposome size indicate that Pb^{2+} also significantly increased the diameter of PIP-containing liposomes by 21.00 ± 1.5 nm (Fig. 2B).

Co^{2+} also caused a significant rigidifying effect on PIP alongside a significant decrease of about 10.6 ± 1.4 nm in liposome size (Fig. 2B). While Cd^{2+} and Ni^{2+} also decreased the liposome diameter, their impact

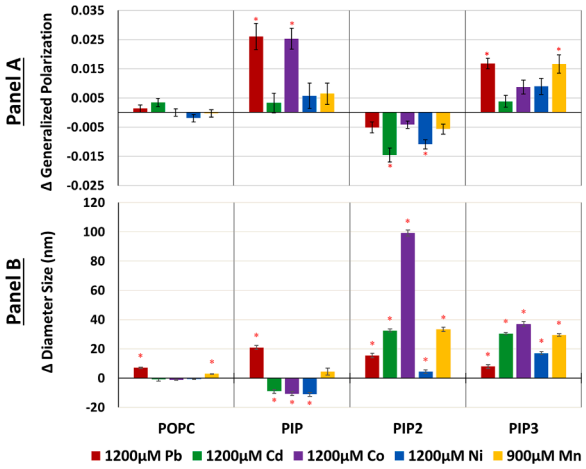

Fig. 2. Change in the generalized polarization (A) and size (B) of PI lipids containing liposomes due to various metals. Panel A) The change in laurdan GP of POPC controls and liposomes containing 1% of either PIP, PIP_2, and PIP_3 upon addition of 1200 μM Pb^{2+} (red), Cd^{2+} (green), Co^{2+} (purple), Ni^{2+} (blue), and 900 μM Mn^{2+} (orange). Panel B) The change in liposome diameter size DLS of POPC controls liposomes containing 1% PIP, PIP_2, and PIP_3 liposomes assessed by DLS at 35°C upon addition of 1200 μM Pb^{2+} (red), Cd^{2+} (green), Co^{2+} (purple), Ni^{2+} (blue), and 900 μM Mn^{2+} (orange). Error bars note standard deviation of triplicates with red asterisks for statistical significance with a 95% confidence interval from the control non-metal reading.

was not enough to affect the overall average membrane fluidity as detected by laurdan (Fig. 2A).

The corresponding BAM images show limited changes to the lateral organization of PIP-containing films with metals at a physiologically relevant surface pressure of ~30 mN/m, representing monolayer-bilayer equivalence in lipid packing [58, 59] (Fig. 3). Limited cluster formation was seen for Cd^{2+} (Fig. 3) and less for Mn^{2+} (images not shown). In terms of Pb^{2+}, void-like defects represented by the dark spots were present in the more homogenous film (Fig. 3A inserts).

POPC + 1 mol% PIP_2 (DOPI(4,5)P_2)

In contrast to the monophosphorylated PIP, significant fluidizing effects were observed in PIP_2 containing systems, indicated by decreased ΔGP values. This is the only fluidization effect observed in all systems whereby Cd^{2+} and Ni^{2+} caused the most significant changes with ΔGP values of -0.015 ± 0.002 and -0.011 ± 0.002, respectively (Fig. 2A).

In terms of the metal effects on liposome size, Co^{2+} had the strongest impact by almost doubling the size with a radius increase of 214 ± 5 nm (change in diameter size of 99 ± 2 nm) (Fig. 2B). This could suggests aggregation or large scale fusions as reported for phosphatidylserine liposomes with Ca^{2+} [73] and Cd^{2+} [18]. The Co^{2+} induced change was the most significant alteration whereas Cd^{2+} and Mn^{2+} effects are lower but close to the estimated fusion size range. Size changes for Pb^{2+} of about 15.5 ± 1.5 nm reflect membrane swelling.

In terms of lateral film organization, Pb^{2+} and Co^{2+} induced domain cluster formation with increased monolayer protrusions (Fig. 3B). Additionally, Co^{2+} appears to result in phase separation (Fig. 3A). In PIP_2 metal free systems, no phase separation was observed. This significant Co^{2+} induced clustering in the outer leaflet of liposomes as seen in monolayer studies could facilitate interactions between liposomes, potentially leading to fusion (Fig. 2B).

POPC + 1 mol% PIP_3 (DOPI(3,4,5)P_3)

ΔGP results show rigidification effects whereby Pb^{2+} and Mn^{2+} showed the strongest impact with similar ΔGP values of +0.02 ± 0.002 and +0.02 ± 0.003, respectively, for both metals (Fig. 2B). Co^{2+}, Ni^{2+} and Cd^{2+} resulted in not statistically significant ΔGP values (Fig. 2A).

All metals caused a significant increase in liposome sizes (Fig. 2B). This is supported by the fact that the structure of PIP_3 allows for the 4'-phosphate to be readily accessible at the membrane interface with the most negative surface charge compared to PIP and PIP_2 [74]. This facilitates the binding of divalent metals that can result in membrane swelling or fusion. The largest increase was observed for Co^{2+} with 37 ± 1.5 nm, followed by Cd^{2+} and Mn^{2+} with 30.5 ± 1 nm and 29.5 ± 1 nm, respectively. These increases are within the range of membrane fusion, including slightly lower values for Ni^{2+} with an increase of 17 ± 1 nm. The weakest metal impact on liposome size was induced by Pb^{2+} with only 8 ± 1 nm increase.

In terms of the lateral organization, all metals induced lipid clustering in PIP_3 containing systems (Fig. 4). The most significant effects induced by Pb^{2+} and Ni^{2+} are shown in Figure 3 as 3D images. Pb^{2+} shows phase separation and domain cluster formation indicated by the bright spikes in the insert for the Pb^{2+} image (Fig. 3). The effect of Ni^{2+} on the PIP_3 systems is the most pronounced and comparable to the impact of Co^{2+} on PIP_2 by inducing large scale phase separation (Fig. 4). However, Co^{2+} did have a strong effect on PIP_3 similar to that caused by Pb^{2+} in the form of bright domain clusters. Cd^{2+} resulted in clusters as well but to a much lesser extent. Interestingly, Mn^{2+} had the weakest effect, but it is similar to that caused by Ni^{2+} in terms of inducing phase separation and domain cluster formation (Fig. 4).

Discussion

Adverse health effects as the result of increasing metal exposure can be dated back over the past millennia. Current literature associates metals with extensive toxic effects including cognitive impairment [75, 76], developmental delays [77], oxidative damage [78, 79] and damage to DNA and proteins. While more work has been done on metal interactions with DNA and proteins, lipids constitute half of the cell membranes by weight [80]. Metal interactions with membranes need to be considered.

Cellular membranes provide subcellular compartmentalization and are essential for both intra-and extracellular trafficking. In addition to structural needs, minor membrane lipids can also perform signaling roles. Thus, certain PPIs were selected for the current study. Any alteration of lipid behavior and membrane organization of PPI containing membranes could be part of the mechanism of metal toxicity.

We have previously shown that laurdan fluorescence is a suitable and sensitive tool to assess metal impact on membrane fluidity in model systems such as various negatively charged phosphatidylserine, phosphatidylglycerol and phosphatidic acid with Co^{2+}, Ni^{2+} [17] and Cd^{2+} and Hg^{2+} [18, 20, 81] . In order to show that these effects were caused by metal binding, zeta potential measurements for metal free controls and changes upon the additions of divalent metal ions showed an increase in zeta potential values for all metals (Fig. S4). While the zeta potential is measured at the hydration layer of the liposome, laurdan inserts into the interface and thus report on metal effects at a deeper location of the sample.

Another potential metal effect is liposome swelling, fusion or aggregation which was assessed by dynamic light scattering as shown for

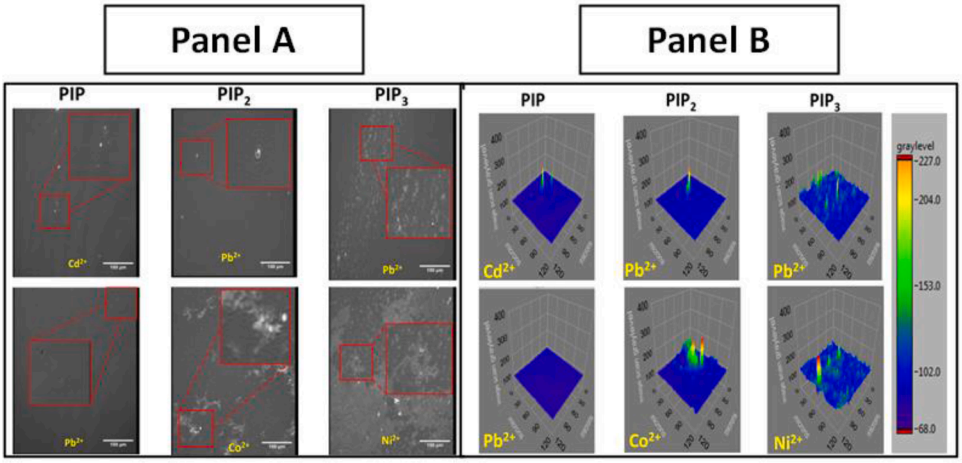

Fig. 3. Effect of some of the metal ions on PI containing monolayers analyzed using BAM. Two images of the most significant effects for each system are displayed. Panel A) Primary metal-induced changes to BAM images of 1% PIP, 1% PIP_2, and 1% PIP_3 monolayers after treatment of 86.2 μM metals (500:1 metal: lipid mol ratio) in 100 mM NaCl at pH 7.4 subphase at room temperature. Inserts indicate zoomed in regions. Panel B) 3D image analysis of zoomed in regions in Panel A. The scale bar represents a qualitative representation of the intensity of domain clusters in height between monolayer and camera. Scale bars correspond to 50 μm.

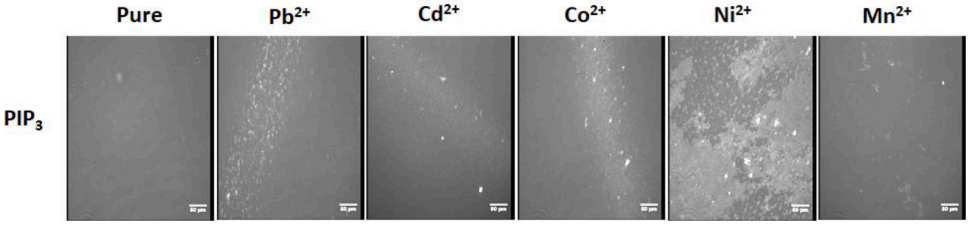

Fig. 4. BAM images of POPC ± 1% PIP3 at 30 mN/m. 3D analysis of Pb^{2+} and Ni^{2+} are shown in Figure 3 above. Each system had a metal lipid mol ratio of 500:1 respectively.

cadmium [18] nickel and cobalt [17].

We have also extensively used Brewster angle microscopy [62] to investigate lateral domain formation in model lipid films [82]. Due to their biophysical investigational benefits, these tools have been combined to examine the impact of metals on PPI containing membranes and our results indicate multiple potentially toxic effects. BAM investigates monolayers spread at the air water interface which were also analyzed by surface pressure-area isotherms [62, 83, 84] (Fig. S5), which also shows moderate increases in overall molecular areas, which is not unexpected when considering how relatively few negatively charged PIs are targets for divalent ions. These films can also be analyzed in terms of the compressibility modulus which is a measure of film fluidity/rigidity [55-57]. Data in Fig. S6 and Fig. S7 confirm trends of film rigidification/fluidization as discussed in detail for the GP analysis.

POPC was used as a matrix as it is the main mammalian structural membrane component. In addition, this lipid showed very limited or no relevant interactions in previous studies with Cd^{2+}, Hg^{2+}, Ni^{2+} and Co^{2+} [17, 18, 81] as well as very limited ΔGP changes for all 5 metals in this work (Fig. 2A). While the average molecular areas and compressibility moduli are averages across the entire system, the GP analysis is focused on dyes in closer proximity to the PI lipids as the metal interactions site. Moreover, BAM images show local membrane architecture when the samples is passed by the laser beam. Localized metal induced effects will be biologically more relevant when they impact the spatiotemporal function of membranes. Thus, the focus was on ΔGP and BAM images.

POPC metal interactions with 1 mol% PIP (DOPI(4)P)

PIP is phosphorylated at the 4' position on the inositol ring of the PI lipid's headgroup (Fig. 1). A ^{31}P NMR study reported a -2 to -3 charge distribution for PIP due to possible charge neutralization at physiological pH in 20 mM Tris-maleate 5 mM EDTA 100 mM NaCl [45]. The orientation of the head group determines the accessibility of PIs for metal binding [85]. While the exact positioning of the phosphates relative to the bilayer plane is still unresolved, ^{1}H NMR experiments assessing the orientation of the inositol ring -OH groups reported that the 3' position is the closest to the membrane backbone, followed by 5' whereas position 4' has the outermost location [3]. Neutron diffraction studies also suggested an orientation of PIP with the 3' OH group positioned down to allow intermolecular hydrogen bonds with neighboring phosphates so the charged 4' phosphate is available for electrostatic interactions with the positive choline groups of PC lipids [86]. This may enhance the favorable hydrogen bonding between axial 2' OH groups with neighboring lipid phosphates as well [87].

The pronounced increase in ΔGP value by Pb^{2+} (Fig. 2A) as well as the increase in liposome size (Fig. 2B) could be due to the small hydrated radius of Pb^{2+} (4.01 Å) [88] and its high electronegativity (2.2) [89] (Table 3). These factors may assist in the deeper binding of this metal in the lipid membrane towards the backbone phosphate linker, as depicted in the Fig. 1B schematic. This increases the average area of the lipid head group due to increased water penetration and subsequent swelling. In addition, a disruption of PI hydrogen bonding network is possible as Pb^{2+} is the only metal to form an appreciable amount of hydroxide species, which are present at around 14% [66] under our experimental conditions (Table 1).

Co^{2+} binding to the external 4' position also induced significant membrane rigidity (Fig. 2A) in the glycerol backbone region however, the concomitant reduction in the liposome size (Fig. 2B) also suggests tighter lipid packing because of membrane binding. Comparatively to Pb^{2+}, the larger hydrated radius (4.23 Å) [88] and lower electronegativity (1.84) [89] (Table 3) of Co^{2+} could result in interactions more externally to the membrane. As the prevailing species of Co^{2+} is divalent (Table 1), these factors may draw the negatively charged lipids together for a rigidifying effect.

Cd^{2+} and Ni^{2+} are less likely to impact PIP lipids as they both showed minor insignificant increases in rigidity (Fig. 2A) while their presence caused a general reduction in liposome sizes of 7% and 9%, respectively (Fig. 2B). This suggests that the presence of these metals spatially pack the lipids tighter without adequately affecting membrane fluidity. Mn^{2+} also exhibited a minor insignificant increase in rigidity (Fig. 2A) but without appreciable changes in liposome size. Mn^{2+} has the lowest electronegativity but the largest hydrodynamic radius of these metals [24] (Table 3), which may reduce interactions close to the backbone.

The lateral film organization was investigated at 30 mN/m, which is physiologically relevant to equivalate monolayer pressure to bilayers [64]. No significant changes and only minor domain cluster formation for Cd^{2+} and Mn^{2+} was observed. The only notable observation was the presence of void like defects represented by the dark spots within the homogenous film, (Fig. 3A inserts). While such features have been previously reported for membranes containing minor lipid or protein components [90-92], in our model system such features were only observed in the presence of Pb and not in metal free controls.

POPC metal interactions with 1 mol% PIP_2 (DOPI(4,5)P_2)

PIP_2 carries an overall charge of around -4 due to the added phosphate group on the 5' position and a proton shared with the adjacent phosphomonoester groups [46]. A detailed conformation of PIP_2 has not

Table 3
Tabulated values of the physical-chemical properties of each metal investigated.

Metal	Hydrated radius (Å)[82]	Electronegativity[85,86]	Hard/Soft Acid/Base (HSAB) [98]	Coordination Chemistry [77,99,100]	Essentiality
Pb	4.01	2.33	Soft	Octahedral	Toxic
Cd	4.26	1.69	Soft	Octahedral, Trigonal pyramidal	Toxic
Co	4.23	1.84	Borderline*	Octahedral, Trigonal pyramidal	Essential
Ni	4.04	1.91	Borderline*	Square planar, Octahedral	Uncertain
Mn	4.38	1.55	Borderline*	Octahedral, Trigonal Bipyramidal	Essential

*Borderline means that it is ranked in between hard and soft lewis acids based on HSAB theory.

been determined however a molecular simulation study on head group protrusion found that the average 4' phosphate is 6 Å away from the membrane plane in contrast to 5 Å for 5' phosphate [26, 87].

PIP_2 is involved in interactions with more than 280 proteins using spatiotemporal distributions of PI pools [9]. Any interference to the PI distribution would have localized effects at given time points in the signaling pathways. Fluidization suggests less tight packing and increased areas per molecule. Such effects were reported for PIP_2 in the presence of monovalent ions (Na^+, K^+, Li^+, Cs^+) whereas the opposite effect was reported for Ca^{2+} and to a lesser effect for Mg^{2+} [93]. As PIP_2 is the most abundant signaling molecule, fluidity changes could have detrimental effects on signal transduction pathways [8-10].

While Co^{2+} had strong binding affinity for PIP (Fig. S4) with a minimal change in liposome size (Fig. 2), this transition metal showed limited fluidization but a significant increase in liposome size of 99 ± 2 nm. This suggests rather aggregation than fusion (see Supplementary Material and Fig. S1). The addition of the 5' phosphate may create the perfect coordination site for the hydrodynamic radius of 4.23 Å [88], reported for Co^{2+}, whereas the smaller Pb^{2+} with 4.01 Å [88] can bind to the more accessible 4` phosphate in the case for PIP (Fig. 2). Atomic radii as well as differences in the preferred coordination complexes will define the outcome of metal binding to the 4' and/or 5' phosphates. For Co^{2+}, the effect would be inter-liposomal, explaining the increase in size that is much larger than size estimates for fusion. At the same time, the effect on the lipid packing at the intra-liposomal level was limited as shown by the insignificant fluidization. The most pronounced effects on fluidity were induced by Cd^{2+} and Ni^{2+}.

Cd^{2+} is similar in size to Co^{2+} (4.23 Å), while Ni^{2+} is slightly smaller at 4.04 Å (Table 3). Cadmium speciates under these experimental conditions into $CdCl^+$ and $CdCl_2$ complexes as well as divalent Cd^{2+}, whereas cobalt, manganese and nickel are predominantly divalent ions (Table 1). Cadmium-induced aggregation of negatively charged POPS liposomes has been reported at 0.50 mM Cd^{2+} while Co^{2+} and Ni^{2+} induced less changes [18]. The fluidization effects seen in PIP_2 systems due to Cd^{2+}, Ni^{2+} and to a lesser extent, Mn^{2+}, did also result in a significant liposomal size increases of 28%, 4%, and 29%, respectively, however none of which reached the same extent as with Co^{2+}. Thus, it is not the binding of these metals to a negatively charged lipids, but the specific coordination with PIP_2 that is responsible for these significant effects.

In terms of lateral membrane organization, ion-induced phase separation has been previously reported as Ca^{2+}-induced solid phase of PS and a fluid phase of PC separation in PC/PS systems [94] as well as phase separation of PGs in PC/PG systems [95]. In addition, the ability of cations to induce changes to lateral organization of PIP_2 has also been observed [85, 94, 96, 97]. MD simulations and lipid monolayer experiments on PIP_2 domain cluster formation has been reported using Ca^{2+} and Mg^{2+} as these metals were able to condense PIP_2-containing membranes which may involve changes in packing geometry and hydration enthalpy [85, 96]. Ca^{2+} interactions with PIP_2 changed the ionization state leading to PIP_2 domain formation [85, 98]. It was found that Ca^{2+} has the ability to cluster up to 3 PIP_2 molecules based on the law of matching water affinities and where the electrostatic interactions are strong enough to overcome the dehydration energy and the resulting entropic effects [32, 63]. In addition, hydrogen bonding networks were proposed to change the charge distribution in PIP_2 leading to mixed domains of PI and PIP_2 [99]. The effects were lipid specific where PE in mixtures of PI/PIP_2/PE induced increased hydrogen bonding and ionization exhibiting a stronger effect than PS in PI/PIP_2/PS which the authors attributed to demixing [99]. In contrast, PC, which can't hydrogen bond in comparison to PE and PS, resulted in fluid/fluid demixing in PI/PIP_2/PC systems [99].

Recently, PIP_2 cluster formation at 0.02 - 0.05 mol% was demonstrated by highly sensitive fluorescence energy transfer experiments. These results were also independent of the acyl chain composition. Moreover, other lipids like PC, PE, PS or PI did not form co-clusters, but PPIs did [100]. Cholesterol and PI enhanced the trends. These findings show that the bulk lipid composition affects cluster formation.

Considering PIP_2 concentrations in the cytosolic leaflet of the plasma membranes is 1-2 %, most of these lipids could be present in clusters. Tighter metal induced packing and concomitantly reduced membrane fluidity between leaflets can induce curvature [32]. Indeed, bulge formation has been reported for supported monolayers of PIP_2 in the presence of Ca^{2+} [97]. Disruptions caused by the clustering of PIP_2 may lead to either enhanced or decreased function of proteins that interact with PIP_2 [63]. Under our experimental conditions, Pb^{2+} and Co^{2+} induced domain cluster formation with increased monolayer protrusions (Fig. 3B). Especially the presence of Co^{2+} results in phase separation in addition to cluster formation (Fig. 3A). Since these monolayers only contain 1% PIP_2, the observed clusters must include significant amounts of POPC as well. It is interesting to note that Co^{2+} induced the most pronounced effect in the monolayer systems and by far the biggest increases in liposome size yet no effect was seen in the laurdan studies. Cluster formation and negative curvature was reported for Ca^{2+} in giant unilamellar vesicles potentially leading to phase separation [74]. Therefore, similar forces could be driving the clustering and phase separation effects seen here with PIP_2.

A direct comparison between bilayer ΔGP data and monolayer data is not straightforward [96, 97]. The single monolayer plane provides a very precise lipid composition and can be used as a model for the outer leaflet of a membrane exposed to metals in the extracellular space. Nevertheless, certain factors need to be considered such as the bilayer curvature which is absent in monolayers, which will change intermolecular distances and angles, and impact metal binding although PIP_2 clusters have been reported for monolayers models [63] and bilayers alike [100].

POPC metal interactions with 1 mol% PIP_3 (DOPI(3,4,5)P_3)

The last lipid analyzed was PIP_3 which is formed *in vivo* by the phosphorylation of PIP_2 lipid at the 3' position (Fig. 1). It is also the largest and most negative of all the PPIs with a charge of -5 due to charge localization of the negative charge on the phosphate group [46]. Moreover, a comprehensive analysis by NMR based on chemical shifts demonstrated that the charge at the 4' was more negative between pH 5 – 7 than 3' and 5' positions [74].

The cellular PIP_3 pool is very dynamic and its regulation is tightly controlled to ensure availability [26]. Signaling abnormalities in its pathway have been linked to a variety of diseases including cancer, diabetes, cardiovascular disease, and various inflammatory disorders [35].

The most pronounced changes in membrane rigidification were observed for Pb^{2+} and Mn^{2+} which also resulted in a significant liposomal size increase of 7 % and 27 %, respectively. Despite the metal ions sharing a preferred coordination complex of octahedral geometry, manganese mainly speciates into divalent ions whereas lead is found as $PbCl^+$, Pb^{2+} and $PbOH^+$ under these experimental conditions (Table 1). Moreover, there is a significant difference in the atomic radius whereby Mn^{2+} is larger (4.35 Å) than Pb^{2+} (4.01 Å) [24]. Atomic radii as well as differences in the metal species charges will define the outcome of metal binding to the highly negative PIP_3. While both metals are equally rigidifying the membrane, Mn^{2+} induces larger lipid packing alterations upon metal coordination.

More moderate ΔGP increases in rigidity were determined for Co^{2+} (4.24 Å) and Ni^{2+} (4.06 Å) (Fig. 2A). The preferred complexation geometry of both Co^{2+} and Ni^{2+} is octahedral. However, both of these metals can adopt a different complexation geometry, namely trigonal bipyramidal and square planar for Co^{2+} and Ni^{2+} respectively (Table 3). Both Co^{2+} and Ni^{2+} coordination to the phosphate groups of PIP_3 show only moderate effects on membrane fluidity but have a significant impact on liposome size of 34 % and 15 %, respectively. While the size increase seen with Co^{2+} exceeds the effect of Mn^{2+} in PIP_3, both suggest

potential liposome fusion. The ΔGP of Ni^{2+} was like that seen with Co^{2+} but the size increase is limited suggesting liposomal swelling. Although this size increase was double that seen for Pb^{2+} system, it did not cause a significant rigidifying effect as seen with Pb^{2+} matrices (Fig. 2).

Finally, Cd^{2+} does not induce appreciable changes in membrane fluidity (Fig. 2A) but the liposome size increase of 28 % is the second largest effect in this system followed closely by Mn^{2+} (27 %). Cd speciates into $CdCl^{+}$ and $CdCl_2$ complexes as well as Cd^{2+} [18] and we have previously reported Cd^{2+} size changes for negatively charged liposomes. In term of size, Cd^{2+} (4.26 Å) is very similar to Co^{2+} (4.24 Å) but smaller than Mn^{2+} (4.35 Å) with a preference for octahedral complexes. The octahedral geometry is suggested to be a preferred coordination complexes to define the outcome of metal binding to PIP_3.

An inverse correlation between electronegativity and cation polarizability have been reported, as lower values of the former result in increases of the latter [101]. In terms of the metals investigated here, Pb^{2+}, Co^{2+} and Ni^{2+} have similar electronegativities around 1.9 followed by Cd (1.6) and Mn (1.55) (Table 3). The relative minor differences are less likely to explain the observed differences and more work will be required to investigate other parameters like coordination geometry.

In terms of the lateral organization, all metals induced lipid domain clustering in PIP_3-containing systems (Fig. 4). The most significant effects were induced by Pb^{2+} and Ni^{2+} as shown in Figure 4. The effect of Ni^{2+} on PIP_3 systems was similar but more pronounced than the impact of Co^{2+} on PIP_2, in inducing phase separation in the monofilm into liquid expanded and liquid condensed phases (Fig. 3). Factors separating Pb^{2+} and Ni^{2+} from the other metals tested are their smaller hydrated radii (4.01 and 4.04 Å, respectively [88]) and the higher electronegativity (2.2 and 1.91, respectively [89]).

Domain formation of PIP_3 [74] in the presence of PI has been proposed due to changes in the protonation states of the phosphates and the impact of hydrogen bonding networks. PE and PI mixtures with PIP_3 were compared whereby PE had a stronger impact on the detailed protonation states leading to higher charges on the phosphates at positions 3' and 5' of PIP_3 [74]. While both lipids can form hydrogen bonds, only PI-induced domains enriched in PI and PIP_3 and these structures, in conjunction with proteins, could serve important signaling roles [74]. Metal ion-induced phase separation for PIP_3 has not been reported before. Moreover, the data suggests that Pb^{2+} and Ni^{2+} metals can induce phase separation in monofilms containing only 1 mol% PIP_3 as the only charged lipid within a matrix of zwitterionic phosphatidylcholine.

Conclusion

The mechanism of metal toxicity is still not fully understood. Many different aspects of interactions with biologically relevant macromolecules may contribute, including the increasingly recognized role of lipids for metal toxicity [17-21, 81, 102]. The data and references in this manuscript emphasize the role of metal induced lipid-lipid interactions.

Model systems reflecting the relatively low abundance of PPIs were used to compare the impact of toxic (Pb^{2+} and Cd^{2+}), physiologically not relevant transition metals (Ni^{2+}), and metals that serve physiological roles (Co^{2+}, Mn^{2+}). The absolute GP changes were small as expected considering the very low PI content but reflected significant metal-induced rigidification for PIP and PIP_3 and fluidification in PIP_2. Liposome size increases were most pronounced for Co^{2+}, followed by Cd^{2+} and Mn^{2+} in both PIP_2 and PIP_3 systems.

The most striking changes were observed with the lateral membrane organization. Previous work has suggested PIP_2 and PIP_3 domains form in the presence of PI [74, 99]. In addition, the stabilization of PI domains by cholesterol has been reported due to hydrogen bonding contributions of the sterol's hydroxyl group [103]. Moreover, the biologically relevant ions Ca^{2+} and Mg^{2+} have been known to induce localized domains of phosphoinositides [85, 97] where the spatiotemporally controlled domains serve important signaling physiological roles.

The presented data suggests that the investigated metals can interfere with biologically important and highly regulated signaling events by inducing new clusters that would not form otherwise. In addition to lipid-metal specific events as reported here, it must be emphasized that metals always occur as mixtures [78] and competing effects have been reported for Cd^{2+} and Hg^{2+}[19].

A wide and diverse range of metal effects on the selected phosphoinositides were observed and many factors including but are not limited to the hydration radii [88], electronegativity [89], complex geometry [104-107], as well as the solvation free energy [108, 109] may play a role. Much more work will be necessary to better understand these and other factors in order to gain a conclusive biophysical analysis.

Nevertheless, metal-based toxicity due to altered or impaired lateral lipid domain organization or mobility and potentially resulting detrimental impact on signaling events is a concerning specter with far reaching implications that requires more scientific attention.

Author Contributions

RM and EP designed research; RM and WD performed research; RM and WD analyzed the data; RM, WD, KS and EP wrote the paper.

Declaration of Competing Interest

The authors declare that they have no conflicts of interest with the contents of this article. Supplementary Information accompanies this paper.

Acknowledgment

This work is supported by an NSERC Discovery Grant to EJP and a Queen Elizabeth (II) Doctoral Scholarship to WD.

Supplementary materials

Supplementary material associated with this article can be found, in the online version, at doi:10.1016/j.bbadva.2021.100021.

References

[1] M.J. Berridge, R.F. Irvine, Inositol phosphates and cell signalling, Nature 341 (6239) (1989) 197–205.
[2] R.H. Michell, C. Kirk, S. Maccallum, P. Hunt, Inositol lipids: receptor-stimulated hydrolysis and cellular lipid pools, Philos. Trans. R. Soc. Lond. B Biol. Sci. 320 (1199) (1988) 239–246.
[3] R.J. Bushby, S.J. Byard, P.M. Hansbro, D.G. Reid, The conformational behaviour of phosphatidylinositol, Biochimica et Biophysica Acta (BBA)-Lipids and Lipid Metabolism 1044 (2) (1990) 231–236.
[4] K. D'Souza, R.M. Epand, Enrichment of phosphatidylinositols with specific acyl chains, Biochimica et Biophysica Acta (BBA)-Biomembranes 1838 (6) (2014) 1501–1508.
[5] D.G. Capelluto, Lipid-mediated protein signaling, Springer, 2013.
[6] T. Balla, Phosphoinositides: tiny lipids with giant impact on cell regulation, Physiol. Rev. 93 (3) (2013) 1019–1137.
[7] J. Tan, J.A. Brill, Cinderella story: PI4P goes from precursor to key signaling molecule, Crit. Rev. Biochem. Mol. Biol. 49 (1) (2014) 33–58.
[8] D.H. Carney, D.L. Scott, E.A. Gordon, E.F. Labelle, Phosphoinositides in mitogenesis: neomycin inhibits thrombin-stimulated phosphoinositide turnover and initiation of cell proliferation, Cell 42 (2) (1985) 479–488.
[9] B. Catimel, C. Schieber, M. Condron, H. Patsiouras, L. Connolly, J. Catimel, E. C. Nice, A.W. Burgess, A.B. Holmes, The PI (3, 5) P2 and PI (4, 5) P2 Interactomes, J. Proteome Res. 7 (12) (2008) 5295–5313.
[10] B.-C. Suh, B. Hille, PIP2 is a necessary cofactor for ion channel function: how and why? Annu. Rev. Biophys. 37 (2008) 175–195.
[11] S. McLaughlin, J. Wang, A. Gambhir, D. Murray, PIP2 and proteins: interactions, organization, and information flow, Annu. Rev. Biophys. Biomol. Struct. 31 (1) (2002) 151–175.
[12] G. Van Meer, D.R. Voelker, G.W. Feigenson, Membrane lipids: where they are and how they behave, Nat. Rev. Mol. Cell Biol. 9 (2) (2008) 112–124.
[13] S. Schmitt, L.C. Castelvetri, M. Simons, Metabolism and functions of lipids in myelin, Biochimica et Biophysica Acta (BBA)-Molecular and Cell Biology of Lipids 1851 (8) (2015) 999–1005.

[14] R.S. Vest, L.J. Gonzales, S.A. Permann, E. Spencer, L.D. Hansen, A.M. Judd, J. D. Bell, Divalent cations increase lipid order in erythrocytes and susceptibility to secretory phospholipase A2, Biophys. J. 86 (4) (2004) 2251–2260.
[15] M. Suwalsky, F. Villena, B. Norris, Y. Cuevas, C. Sotomayor, P. Zatta, Effects of lead on the human erythrocyte membrane and molecular models, J. Inorg. Biochem. 97 (3) (2003) 308–313.
[16] M. Suwalsky, F. Villena, B. Norris, F. Cuevas, C. Sotomayor, Cadmium-induced changes in the membrane of human erythrocytes and molecular models, J. Inorg. Biochem. 98 (6) (2004) 1061–1066.
[17] J. Umbsaar, E. Kerek, E.J. Prenner, Cobalt and nickel affect the fluidity of negatively-charged biomimetic membranes, Chem. Phys. Lipids 210 (2018) 28–37.
[18] E.M. Kerek, E.J. Prenner, Inorganic cadmium affects the fluidity and size of phospholipid based liposomes, Biochimica et Biophysica Acta (BBA)-Biomembranes 1858 (12) (2016) 3169–3181.
[19] E. Kerek, M. Hassanin, E.J. Prenner, Inorganic mercury and cadmium induce rigidity in eukaryotic lipid extracts while mercury also ruptures red blood cells, Biochimica et Biophysica Acta (BBA)-Biomembranes 1860 (3) (2018) 710–717.
[20] M. Hassanin, E. Kerek, M. Chiu, M. Anikovskiy, E.J. Prenner, Binding affinity of inorganic mercury and cadmium to biomimetic erythrocyte membranes, J. Phys. Chem. B 120 (50) (2016) 12872–12882.
[21] B.J. Payliss, M. Hassanin, E.J. Prenner, The structural and functional effects of Hg (II) and Cd (II) on lipid model systems and human erythrocytes: A review, Chem. Phys. Lipids 193 (2015) 36–51.
[22] D.L. Jones, L.V. Kochian, Aluminum interaction with plasma membrane lipids and enzyme metal binding sites and its potential role in Al cytotoxicity, FEBS Lett. 400 (1) (1997) 51–57.
[23] V. Karri, M. Schuhmacher, V. Kumar, Heavy metals (Pb, Cd, As and MeHg) as risk factors for cognitive dysfunction: A general review of metal mixture mechanism in brain, Environ. Toxicol. Pharmacol. 48 (2016) 203–213.
[24] K. Sule, J. Umbsaar, E.J. Prenner, Mechanisms of Co, Ni, and Mn toxicity: From exposure and homeostasis to their interactions with and impact on lipids and biomembranes, Biochimica et Biophysica Acta (BBA)-Biomembranes (2020), 183250.
[25] M.D. Garrick, S.T. Singleton, F. Vargas, H. Kuo, L. Zhao, M. Knöpfel, T. Davidson, M. Costa, P. Paradkar, J.A. Roth, DMT1: which metals does it transport? Biol. Res. 39 (1) (2006) 79–85.
[26] Z. Li, R.M. Venable, L.A. Rogers, D. Murray, R.W. Pastor, Molecular dynamics simulations of PIP2 and PIP3 in lipid bilayers: determination of ring orientation, and the effects of surface roughness on a Poisson-Boltzmann description, Biophys. J. 97 (1) (2009) 155–163.
[27] D.R. Slochower, P.J. Huwe, R. Radhakrishnan, P.A. Janmey, Quantum and all-atom molecular dynamics simulations of protonation and divalent ion binding to phosphatidylinositol 4, 5-bisphosphate (PIP2), J. Phys. Chem. B 117 (28) (2013) 8322–8329.
[28] M.R. Wenk, L. Lucast, G. Di Paolo, A.J. Romanelli, S.F. Suchy, R.L. Nussbaum, G. W. Cline, G.I. Shulman, W. McMurray, P. De Camilli, Phosphoinositide profiling in complex lipid mixtures using electrospray ionization mass spectrometry, Nat. Biotechnol. 21 (7) (2003) 813–817.
[29] E. Delage, J. Puyaubert, A. Zachowski, E. Ruelland, Signal transduction pathways involving phosphatidylinositol 4-phosphate and phosphatidylinositol 4, 5-bisphosphate: convergences and divergences among eukaryotic kingdoms, Prog. Lipid Res. 52 (1) (2013) 1–14.
[30] R.B. Gennis, Biomembranes: molecular structure and function, Springer Science & Business Media, 2013.
[31] M.A. Lemmon, Membrane recognition by phospholipid-binding domains, Nat. Rev. Mol. Cell Biol. 9 (2) (2008) 99–111.
[32] R.P. Bradley, D.R. Slochower, P.A. Janmey, R. Radhakrishnan, Divalent cations bind to phosphoinositides to induce ion and isomer specific propensities for nano-cluster initiation in bilayer membranes, R. Soc. Open Sci. 7 (5) (2020), 192208.
[33] M.E. Gardocki, N. Jani, J.M. Lopes, Phosphatidylinositol biosynthesis: biochemistry and regulation, Biochimica et Biophysica Acta (BBA)-Molecular and Cell Biology of Lipids 1735 (2) (2005) 89–100.
[34] C. Nasuhoglu, S. Feng, J. Mao, M. Yamamoto, H.L. Yin, S. Earnest, B. Barylko, J. P. Albanesi, D.W. Hilgemann, Nonradioactive analysis of phosphatidylinositides and other anionic phospholipids by anion-exchange high-performance liquid chromatography with suppressed conductivity detection, Anal. Biochem. 301 (2) (2002) 243–254.
[35] R.D. Riehle, S. Cornea, A. Degterev, Role of phosphatidylinositol 3, 4, 5-trisphosphate in cell signaling. Lipid-mediated Protein Signaling, Springer, 2013, pp. 105–139.
[36] R.A. Currie, K.S. Walker, A. Gray, M. Deak, A. Casamayor, C.P. Downes, P. Cohen, D.R. Alessi, J. Lucocq, Role of phosphatidylinositol 3, 4, 5-trisphosphate in regulating the activity and localization of 3-phosphoinositide-dependent protein kinase-1, Biochem. J. 337 (3) (1999) 575–583.
[37] R. Levin, S. Grinstein, D. Schlam, Phosphoinositides in phagocytosis and macropinocytosis, Biochimica Et Biophysica Acta (BBA)-Molecular and Cell Biology of Lipids 1851 (6) (2015) 805–823.
[38] J. Gailer, Arsenic–selenium and mercury–selenium bonds in biology, Coord. Chem. Rev. 251 (1–2) (2007) 234–254.
[39] J.O. Nriagu, A history of global metal pollution, Science 272 (5259) (1996), 223-223.
[40] D.G. Barceloux, D. Barceloux, Cobalt, J. Toxicol. Clin. Toxicol. 37 (2) (1999) 201–216.
[41] D.G. Barceloux, D. Barceloux, Nickel, J. Toxicol. Clin. Toxicol. 37 (2) (1999) 239–258.
[42] J. Godt, F. Scheidig, C. Grosse-Siestrup, V. Esche, P. Brandenburg, A. Reich, D. A. Groneberg, The toxicity of cadmium and resulting hazards for human health, J. Occup. Med. Toxicol. 1 (1) (2006) 1–6.
[43] C.D. Toscano, T.R. Guilarte, Lead neurotoxicity: from exposure to molecular effects, Brain Res. Rev. 49 (3) (2005) 529–554.
[44] J.C. Fuller, M. Martinez, R.C. Wade, On calculation of the electrostatic potential of a phosphatidylinositol phosphate-containing phosphatidylcholine lipid membrane accounting for membrane dynamics, PLoS One 9 (8) (2014), e104778.
[45] P.A. van Paridon, B. de Kruijff, R. Ouwerkerk, K.W. Wirtz, Polyphosphoinositides undergo charge neutralization in the physiological pH range: a 31P-NMR study, Biochimica et Biophysica Acta (BBA)-Lipids and Lipid Metabolism 877 (1) (1986) 216–219.
[46] E.E. Kooijman, K.E. King, M. Gangoda, A. Gericke, Ionization properties of phosphatidylinositol polyphosphates in mixed model membranes, Biochemistry 48 (40) (2009) 9360–9371.
[47] A.B. Santamaria, S.I. Sulsky, Risk assessment of an essential element: manganese, J. Toxicol. Environ. Health Part A 73 (2–3) (2010) 128–155.
[48] S.J. Stohs, D. Bagchi, Oxidative mechanisms in the toxicity of metal ions, Free Radic. Biol. Med. 18 (2) (1995) 321–336.
[49] R.V. Stahelin, J.L. Scott, C.T. Frick, Cellular and molecular interactions of phosphoinositides and peripheral proteins, Chem. Phys. Lipids 182 (2014) 3–18.
[50] A. Gericke, Is calcium fine-tuning phosphoinositide-mediated signaling events through clustering? Biophys. J. 114 (11) (2018) 2483–2484.
[51] A. Shewan, D.J. Eastburn, K. Mostov, Phosphoinositides in cell architecture, Cold Spring Harb. Perspect. Biol. 3 (8) (2011) a004796.
[52] A. Zachowski, Phospholipids in animal eukaryotic membranes: transverse asymmetry and movement, Biochem. J. 294 (1) (1993) 1–14.
[53] C.M. Ferreira, I.S. Pinto, E.V. Soares, H.M. Soares, (Un) suitability of the use of pH buffers in biological, biochemical and environmental studies and their interaction with metal ions–a review, RSC Adv. 5 (39) (2015) 30989–31003.
[54] T. Parasassi, E.K. Krasnowska, L. Bagatolli, E. Gratton, Laurdan and Prodan as polarity-sensitive fluorescent membrane probes, J. Fluoresc. 8 (4) (1998) 365–373.
[55] R.E. Brown, H.L. Brockman, Using monomolecular films to characterize lipid lateral interactions, Lipid Rafts, Springer, 2007, pp. 41–58.
[56] G.L. Gaines, Insoluble monolayers at liquid-gas interfaces, (1966).
[57] M. Broniatowski, M. Flasiński, P. Dynarowicz-Łątka, J. Majewski, Grazing incidence diffraction and X-ray reflectivity studies of the interactions of inorganic mercury salts with membrane lipids in Langmuir monolayers at the air/water interface, J. Phys. Chem. B 114 (29) (2010) 9474–9484.
[58] H. Brockman, Lipid monolayers: why use half a membrane to characterize protein-membrane interactions? Curr. Opin. Struct. Biol. 9 (4) (1999) 438–443.
[59] A. Blume, A comparative study of the phase transitions of phospholipid bilayers and monolayers, Biochimica et Biophysica Acta (BBA)-Biomembranes 557 (1) (1979) 32–44.
[60] P. Dynarowicz-Łątka, A. Dhanabalan, O.N. Oliveira Jr, Modern physicochemical research on Langmuir monolayers, Adv. Colloid Interface Sci. 91 (2) (2001) 221–293.
[61] A.D. Petelska, M. Naumowicz, The effect of divalent ions on L-α-phosphatidylcholine from egg yolk monolayers at the air/water interface, JBIC J. Biol. Inorg. Chem. 22 (8) (2017) 1187–1195.
[62] W. Daear, M. Mahadeo, E.J. Prenner, Applications of Brewster angle microscopy from biological materials to biological systems, Biochimica et Biophysica Acta (BBA)-Biomembranes 1859 (10) (2017) 1749–1766.
[63] K. Han, A. Gericke, R.W. Pastor, Characterization of specific ion effects on PI (4, 5) P2 clustering: molecular dynamics simulations and graph-theoretic analysis, J. Phys. Chem. B 124 (7) (2020) 1183–1196.
[64] D. Marsh, Lateral pressure in membranes, Biochimica et Biophysica Acta (BBA)-Rev. Biomembranes 1286 (3) (1996) 183–223.
[65] R. Demel, W. Geurts van Kessel, R. Zwaal, B. Roelofsen, L. Van Deenen, Relation between various phospholipase actions on human red cell membranes and the interfacial phospholipid pressure in monolayers, Biochimica et Biophysica Acta (BBA)-Biomembranes 406 (1) (1975) 97–107.
[66] J. Gustafsson, Visual MINTEQ Version 3.1: A Windows version of MINTEQA2, 2011.
[67] B.N. Ames, [10]Assay of inorganic phosphate, total phosphate and phosphatases. Methods in enzymology, Elsevier, 1966, pp. 115–118.
[68] C.C. Logisz, J.S. Hovis, Effect of salt concentration on membrane lysis pressure, Biochimica et Biophysica Acta (BBA)-Biomembranes 1717 (2) (2005) 104–108.
[69] F. Sajadi, C.N. Rowley, Simulations of lipid bilayers using the CHARMM36 force field with the TIP3P-FB and TIP4P-FB water models, PeerJ 6 (2018) e5472.
[70] N. Kučerka, M.-P. Nieh, J. Katsaras, Fluid phase lipid areas and bilayer thicknesses of commonly used phosphatidylcholines as a function of temperature, Biochimica et Biophysica Acta (BBA)-Biomembranes 1808 (11) (2011) 2761–2771.
[71] D. Marquardt, B. Geier, G. Pabst, Asymmetric lipid membranes: towards more realistic model systems, Membranes 5 (2) (2015) 180–196.
[72] O. Poulsen, J.M. Christensen, E. Sabbioni, M. Van der Venne, Trace element reference values in tissues from inhabitants of the European Community. V. Review of trace elements in blood, serum and urine and critical evaluation of reference values for the Danish population, Sci. Total Environ. 141 (1–3) (1994) 197–215.
[73] D. Papahadjopoulos, G. Poste, B. Schaeffer, W. Vail, Membrane fusion and molecular segregation in phospholipid vesicles, Biochimica et Biophysica Acta (BBA)-Biomembranes 352 (1) (1974) 10–28.

[74] Z.T. Graber, J. Thomas, E. Johnson, A. Gericke, E.E. Kooijman, Effect of H-bond donor lipids on phosphatidylinositol-3, 4, 5-trisphosphate ionization and clustering, Biophys. J. 114 (1) (2018) 126–136.
[75] R.A. Goyer, Toxic and essential metal interactions, Annu. Rev. Nutr. 17 (1) (1997) 37–50.
[76] A.P. Neal, T.R. Guilarte, Mechanisms of lead and manganese neurotoxicity, Toxicol. Res. 2 (2) (2013) 99–114.
[77] J. Domingo, Metal-induced developmental toxicity in mammals: A review, J. Toxicol. Environ. Health Part A Curr. Issues 42 (2) (1994) 123–141.
[78] V. Andrade, M. Mateus, M. Batoreu, M. Aschner, A.M. Dos Santos, Lead, arsenic, and manganese metal mixture exposures: focus on biomarkers of effect, Biol. Trace Elem. Res. 166 (1) (2015) 13–23.
[79] N. Ercal, H. Gurer-Orhan, N. Aykin-Burns, Toxic metals and oxidative stress part I: mechanisms involved in metal-induced oxidative damage, Curr. Top. Med. Chem. 1 (6) (2001) 529–539.
[80] G.M. Cooper, R.E. Hausman, The cell: Molecular approach, Medicinska naklada, 2004.
[81] E. Kerek, M. Hassanin, W. Zhang, E.J. Prenner, Preferential binding of Inorganic Mercury to specific lipid classes and its competition with Cadmium, Biochimica et Biophysica Acta (BBA)-Biomembranes 1859 (7) (2017) 1211–1221.
[82] M. Patterson, H.J. Vogel, E.J. Prenner, Biophysical characterization of monofilm model systems composed of selected tear film phospholipids, Biochimica et Biophysica Acta (BBA)-Biomembranes 1858 (2) (2016) 403–414.
[83] S. Hénon, J. Meunier, Microscope at the Brewster angle: Direct observation of first-order phase transitions in monolayers, Rev. Sci. Instrum. 62 (4) (1991) 936–939.
[84] D. Hoenig, D. Moebius, Direct visualization of monolayers at the air-water interface by Brewster angle microscopy, J. Phys. Chem. 95 (12) (1991) 4590–4592.
[85] Y.-H. Wang, D.R. Slochower, P.A. Janmey, Counterion-mediated cluster formation by polyphosphoinositides, Chem. Phys. Lipids 182 (2014) 38–51.
[86] J.P. Bradshaw, R.J. Bushby, C.C. Giles, M.R. Saunders, A. Saxena, The headgroup orientation of dimyristoylphosphatidylinositol-4-phosphate in mixed lipid bilayers: a neutron diffraction study, Biochimica et Biophysica Acta (BBA)-Biomembranes 1329 (1) (1997) 124–138.
[87] D. Lupyan, M. Mezei, D.E. Logothetis, R. Osman, A molecular dynamics investigation of lipid bilayer perturbation by PIP2, Biophys. J. 98 (2) (2010) 240–247.
[88] E. Nightingale Jr, Phenomenological theory of ion solvation. Effective radii of hydrated ions, J. Phys. Chem. 63 (9) (1959) 1381–1387.
[89] A. Allred, Electronegativity values from thermochemical data, J. Inorg. Nucl. Chem. 17 (3–4) (1961) 215–221.
[90] B. Maggio, T. Ariga, R.O. Calderón, K.Y. Robert, Ganglioside GD3 and GD3-lactone mediated regulation of the intermolecular organization in mixed monolayers with dipalmitoylphosphatidylcholine, Chem. Phys. Lipids 90 (1–2) (1997) 1–10.
[91] D.C. Carrer, B. Maggio, Transduction to self-assembly of molecular geometry and local interactions in mixtures of ceramides and ganglioside GM1, Biochimica et Biophysica Acta (BBA)-Biomembranes 1514 (1) (2001) 87–99.
[92] G.A. Borioli, B.L. Caputto, B. Maggio, c-Fos and phosphatidylinositol-4, 5-bisphosphate reciprocally reorganize in mixed monolayers, Biochimica et Biophysica Acta (BBA)-Biomembranes 1668 (1) (2005) 41–52.
[93] I. Levental, A. Cebers, P.A. Janmey, Combined electrostatics and hydrogen bonding determine intermolecular interactions between polyphosphoinositides, J. Am. Chem. Soc. 130 (28) (2008) 9025–9030.
[94] S. Ohnishi, T. Ito, Calcium-induced phase separations in phosphatidylserine-phosphatidylcholine membranes, Biochemistry 13 (5) (1974) 881–887.
[95] S. Mittler-Neher, W. Knoll, Ca2+-induced lateral phase separation in black lipid membranes and its coupling to the ion translocation by gramicidin, Biochimica et Biophysica Acta (BBA)-Biomembranes 1152 (2) (1993) 259–269.
[96] W.G. Ellenbroek, Y.-H. Wang, D.A. Christian, D.E. Discher, P.A. Janmey, A.J. Liu, Divalent cation-dependent formation of electrostatic PIP2 clusters in lipid monolayers, Biophys. J. 101 (9) (2011) 2178–2184.
[97] Y.-H. Wang, A. Collins, L. Guo, K.B. Smith-Dupont, F. Gai, T. Svitkina, P. A. Janmey, Divalent cation-induced cluster formation by polyphosphoinositides in model membranes, J. Am. Chem. Soc. 134 (7) (2012) 3387–3395.
[98] Z. Graber, W. Wang, G. Singh, I. Kuzmenko, D. Vaknin, E. Kooijman, Competitive cation binding to phosphatidylinositol-4, 5-bisphosphate domains revealed by X-ray fluorescence, RSC Adv. 5 (129) (2015) 106536–106542.
[99] Z.T. Graber, Z. Jiang, A. Gericke, E.E. Kooijman, Phosphatidylinositol-4, 5-bisphosphate ionization and domain formation in the presence of lipids with hydrogen bond donor capabilities, Chem. Phys. Lipids 165 (6) (2012) 696–704.
[100] Y. Wen, V.M. Vogt, G.W. Feigenson, Multivalent cation-bridged PI (4, 5) P2 clusters form at very low concentrations, Biophys. J. 114 (11) (2018) 2630–2639.
[101] V. Dimitrov, T. Komatsu, Correlation among electronegativity, cation polarizability, optical basicity and single bond strength of simple oxides, J. Solid State Chem. 196 (2012) 574–578.
[102] M.T. Le, M. Hassanin, M. Mahadeo, J. Gailer, E.J. Prenner, Hg-and Cd-induced modulation of lipid packing and monolayer fluidity in biomimetic erythrocyte model systems, Chem. Phys. Lipids 170 (2013) 46–54.
[103] Z. Jiang, R.E. Redfern, Y. Isler, A.H. Ross, A. Gericke, Cholesterol stabilizes fluid phosphoinositide domains, Chem. Phys. Lipids 182 (2014) 52–61.
[104] B. Barszcz, Coordination properties of didentate N, O heterocyclic alcohols and aldehydes towards Cu (II), Co (II), Zn (II) and Cd (II) ions in the solid state and aqueous solution, Coord. Chem. Rev. 249 (21–22) (2005) 2259–2276.
[105] J. Chan, M.E. Merrifield, A.V. Soldatov, M.J. Stillman, XAFS spectral analysis of the cadmium coordination geometry in cadmium thiolate clusters in metallothionein, Inorg. Chem. 44 (14) (2005) 4923–4933.
[106] N.H. Patel, H.M. Parekh, M.N. Patel, Synthesis, characterization and biological evaluation of manganese (II), cobalt (II), nickel (II), copper (II), and cadmium (II) complexes with monobasic (NO) and neutral (NN) Schiff bases, Transition Met. Chem. 30 (1) (2005) 13–17.
[107] M. Ribeiro, M. Domingues, J. Freire, N. Santos, M. Castanho, Translocating the blood-brain barrier using electrostatics, Front. Cell. Neurosci. 6 (2012) 44.
[108] S. Riahi, B. Roux, C.N. Rowley, QM/MM molecular dynamics simulations of the hydration of Mg (II) and Zn (II) ions, Can. J. Chem. 91 (7) (2013) 552–558.
[109] Y. Marcus, Thermodynamics of solvation of ions. Part 5.—Gibbs free energy of hydration at 298.15 K, J. Chem. Soc. Faraday Trans. 87 (18) (1991) 2995–2999.